Polymer Testing 115 (2022) 107719

Contents lists available at ScienceDirect

Polymer Testing

journal homepage: www.elsevier.com/locate/polytest

Sorption dynamics of synthetic fuels and corresponding model mixtures in aged acrylonitrile-butadiene rubber

Benedikt Demmel [a,b,*], Tobias Förster [b], Sebastian Eibl [b]

[a] Universität der Bundeswehr München, Fakultät für Luft- und Raumfahrttechnik, Institut für Mechanik, Werner-Heisenberg-Weg 39, 85579, Neubiberg, Germany
[b] Wehrwissenschaftliches Institut für Werk- und Betriebsstoffe (WIWeB), Institutsweg 1, 85435, Erding, Germany

ARTICLE INFO

Keywords:
Acrylonitrile-butadiene rubber (NBR)
Synthetic fuels
Aging
Swelling
GC/MS
Mechanical testing

ABSTRACT

The sorption dynamics of synthetic aviation fuels, conventional kerosene, and corresponding model mixtures in thermo-oxidatively aged acrylonitrile-butadiene rubber (NBR) are studied. It is found that the diffusion coefficients and equilibrium mass uptakes of fuels and model mixtures in the elastomers are increased for compositions with high aromatics content and decreased for aged elastomers due to increased crosslink densities and polarity. Gas chromatography/mass spectrometry-assisted experiments are used to quantitatively analyze sorption for individual substances in the model mixture with time resolution. Due to strong interactions between the aromatics and the cyano group, the aromatics strongly swell the elastomer especially at the beginning after immersion. In addition, mechanical properties such as hardness, density, elongation, and stress at break are discussed, considering the chemical composition of the fuel and the aging condition of the elastomer. The aging of NBR affects the sorption dynamics of synthetic and conventional fuels similarly and are explained in detail by the model fuel approach.

1. Introduction

Synthetic fuels are attracting considerable interest as alternative energy sources in the aviation sector [1]. Main advantages are their high volumetric energy density and renewable feedstocks [2]. So far, some synthetic fuels blended with kerosene have been certified for civil and military aviation, but more research is needed to promote their safe and widespread use. One of the crucial aspects is a potentially different or adverse interaction between synthetic fuels and construction materials in the aircraft compared to the interaction with conventional kerosene [3,4]. Especially, elastomers in seals, hoses, and tank linings in contact with fuels respond distinctly by swelling [5], extraction of plasticizers [6], and a change in mechanical properties such as hardness or strain. Most studies to date have focused on the interaction of fuels with pristine elastomers. Graham et al. [7] investigated the influence of selected aromatics blended with synthetic jet fuel on volume swelling by correlation with partition coefficients determined by gas chromatography/-mass spectrometry (GC/MS). Usually, the diffusion of fuels into elastomers is studied by sorption experiments, which are carried out gravimetrically [8] and give only mass or volume changes. Blivernitz et al. [9] developed a method for simultaneous and time-resolved quantification of sorption and extraction processes of individual model fuel components and elastomer additives by GC/MS-assisted sorption experiments. Acrylonitrile-butadiene rubber (NBR) is a material typically used for applications involving nonpolar fuels with low aromatics content and is part of many aircraft seals. Over long periods of aircraft service times, especially in the military sector, elastomer properties change. Replacing aged elastomer parts in an aircraft requires considerable effort and consumes resources and money. Consequently, elastomer aging studies that lead to a better estimation of material life contribute to more sustainable use of elastomer components. Accelerated aging of NBR has been studied in detail in various scenarios under air [10], mechanical stress [11], or in liquid media [12,13]. Aging deteriorates the mechanical properties [14], increases the crosslink density [15], and the elastomer is oxidized [16], leading to an increase in the surface free energy [17] and the formation of polar functional groups. Some studies shed light on the degradation mechanisms [18] and the activation energies for the aging processes [19]. This work aims to better understand the interaction of NBR with aviation fuels, especially in aged conditions. Therefore, this work presents a comprehensive investigation of the diffusion processes combined with mechanical testing of thermo-oxidatively aged NBR in contact with liquid media. The focus of

* Corresponding author. Universität der Bundeswehr München, Fakultät für Luft- und Raumfahrttechnik, Institut für Mechanik, Werner-Heisenberg-Weg 39, 85579, Neubiberg, Germany.
E-mail address: benedikt.demmel@unibw.de (B. Demmel).

https://doi.org/10.1016/j.polymertesting.2022.107719
Received 18 May 2022; Received in revised form 12 July 2022; Accepted 22 July 2022
Available online 31 July 2022

the study lies in the detailed description of the sorption of single substances and substance classes by GC/MS in aged elastomers. First, general diffusion dynamics are derived by investigating model fuel mixtures. These findings are applied to the synthetic drop-in fuel ReadiJet™ and the conventional kerosene Jet A-1. The findings contribute to the safe long-term use of elastomers in contact with synthetic aviation fuels.

2. Experimental

2.1. Materials

All experiments were carried out with a carbon black filled acrylonitrile-butadiene rubber (NBR) with an acrylonitrile content of 18 wt% "NBR18", supplied by Deutsches Institut für Kautschuktechnologie (DIK). The detailed composition of the material is given in Table 1 as parts-per-hundred rubber (phr).

Model mixtures (MM) with representative substance classes of aviation fuels such as aromatic, cycloaliphatic, and aliphatic hydrocarbons used for swelling and sorption experiments as well as gas chromatography/mass spectrometry (GC/MS) standard solutions were prepared using analytical grade reagents, namely mesitylene, decalin and dodecane (≥99%, Sigma Aldrich). Their composition and an overview of the investigated fuels is given in Table 2.

The synthetic drop-in jet fuel ReadiJet™, produced by Applied Research Associates, is a complex mixture of hydrocarbons [20,21] with an aromatics content of 21.2 vol% and a density of 0.823 g cm^{-3}. For comparison, a conventional kerosene Jet A-1 with 16.2 vol% aromatics and a density of 0.812 g cm^{-3} was used. Calibration standards for the determination of the aromatics content in sorption experiments by GC/MS were prepared with concentrations ranging from 10 to 90 vol% "AroMix" in an aromatics-free Fischer-Tropsch fuel (CtL) from Sasol. The aromatic solvents "Aromatic 100, 150, and 200″ provided by Exxon were mixed in concentrations of 25, 53, and 22 vol%, respectively, called "AroMix" to match the aromatic composition of a typical JP-8 fuel [22].

2.2. Experiments

Elastomer samples were aged in air in a natural convection heating oven at temperatures of 80 °C for 14, 28, 56, 112, and 224 days, at 100 °C for 7, 14, 28, 42 and 56 days, and at 120 °C for 1, 2, 3, 5, 7, 10, 14 and 28 days. They were then extracted with acetone in a Soxhlet apparatus for 2 days to remove the additives. The sample geometry for the sorption experiments was 20 mm × 10 mm x 1 mm. S2 samples [23] with a thickness of 1.2 mm were used for the mechanical tests.

For swelling experiments, extracted NBR18 samples of approximately 300 mg were immersed in toluene for 7 days at room temperature until swelling equilibrium was reached. The relative error of the threefold measurements was less than 1 %. The elastomer weight fraction w_E was calculated as $w_E = \frac{m_0}{m_{eq}}$, where m_0 is the mass of extracted elastomers and m_{eq} is the equilibrium mass. Gravimetric sorption experiments [8] were used to assess the relative mass change Δm_{grav} of the elastomer samples due to sorption of model mixtures with the absolute mass m_t at time t by $\Delta m_{grav} = \left(\frac{m_t - m_0}{m_0}\right) \cdot 100$ wt%. For this purpose, extracted elastomer samples were stored in screw-cap glasses containing the corresponding model mixtures. Periodically, the samples were taken out, dipped in benzine 40/60 (<1 s), and wiped dry with a paper tissue. After the masses were determined, the samples were returned to their respective storage liquids.

Table 1
Ready-to-use formulation of the investigated NBR18 elastomer.

Component	Content/phr
Perbunan 1846	100
Bis(2-ethylhexyl) phthalate (DEHP)	20
N-(1,3-dimethylbutyl)-*N*′-phenyl-*p*-phenylene diamine (6PPD)	2
Carbon black (type: N550)	60
Zinc oxide	5
Stearic acid	1
Sulfur	2
N-Cyclohexyl-2-benzothiazole sulfenamide (CBS)	1.5
TMTM-80[a]	0.5

[a] 80 % tetramethylthiuram monosulfide, 20 % elastomer binder and dispersing agents.

Table 2
Composition of the fuel-like model mixtures and fuels given in vol%.

Component	Mixture 1 "high aromatics content"	Mixture 2	Mixture 3 "low aromatics content"
Mesitylene	33.3	20	10
Decalin	33.3	20	10
Dodecane	33.3	60	80

Fuel	Aromatics content	Comment
ReadiJet	21.2	Synthetic drop-in fuel
Jet A-1	16.2	Conventional kerosene
CtL	0	Synthetic paraffinic kerosene, aromatics free
AroMix	100	Purely aromatic hydrocarbon mixture (25, 53, and 22 vol% of Aromatic 100, 150 and 200)

For sorption experiments with GC/MS assistance, the weighing step was replaced by punching out small samples of approximately 8 mg from the elastomer, which were then extracted in screw-cap vials with 1 mL acetone. The individual mass uptake Δm of absorbed substances was derived from GC/MS via external calibration and then normalized to the weight of the extracted elastomer m_0 to obtain the relative mass change. Summing Δm for all analytes gives $\Delta m_{GC/MS}$ [9] and is equivalent to Δm_{grav} determined from the gravimetric sorption experiments.

Theoretical sorption curves and diffusion coefficients D, were obtained by iteratively fitting the obtained data using Eq. (1) for one-dimensional diffusion in a plane sheet according to Fick's second law considering the first 12 elements of the infinite series [24]. The relative uptake of liquids at equilibrium is expressed as Δm_{eq} and Δm_t at time t for individual substances and their mixtures or aviation fuels. The specimen thickness h is about 1 mm, and n is the running index.

$$\frac{\Delta m_t}{\Delta m_{eq}} = 1 - \frac{8}{\pi^2} \sum_{n=0}^{11} \left(\frac{1}{(2n+1)^2} \cdot \exp\left(\frac{-(2n+1)^2 \pi^2 D t}{h^2} \right) \right) \quad (1)$$

The aromatics content in the experiments with ReadiJet™ was derived by external calibration with standards of varying amounts of AroMix (vol%) in an aromatics-free Fischer-Tropsch fuel [25]. The intensities I of the mass-to-charge ratios (m/z) of the mass spectra signals characteristic of aliphatic hydrocarbons $I_{m/z,aliph}$ with m/z = 41, 55, 57, 71, 85, 99, 69, 83, 97 and aromatic hydrocarbons $I_{m/z,aro}$ with m/z = 91, 105, 119, 120, 128, 115, 142 were respectively summed up in the retention time range of the fuel. Then, the sum of aliphatic signals ($I_{m/z,aliph}$) was put in relation to the sum ($I_{m/z,sum}$) of aromatic and aliphatic hydrocarbons according to Eq. (2). The $I_{m/z,aliph}/I_{m/z,sum}$ ratio was plotted against the aromatics content v of the standard solutions in vol% to obtain the calibration plot (see Fig. 1). Additives and absorbed species were quantified with external standard solutions of DEHP, 6PPD and model substances in acetone at appropriate concentrations by analyzing them by GC/MS. An Agilent 7890A gas chromatograph coupled with an Agilent 5975 MSD mass spectrometer was used. The column was a 30 m DB-5MS (0.25 mm inner diameter, 0.25 μm film thickness). The GC oven was heated from 50 to 320 °C at 50 K min^{-1} and held at 320 °C for 5 min. The weighing was performed using an analytical balance AG 285 from Mettler Toledo with an accuracy of ±0.1 mg. The GC/MS assisted sorption experiments are applied here in the context of synthetic aviation fuels, but the method is generally also applicable to other

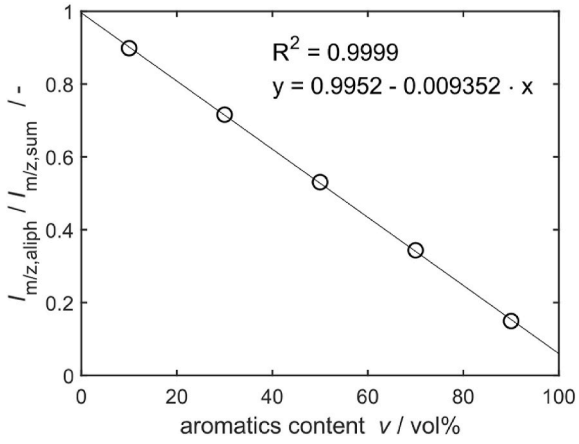

Fig. 1. Calibration curve for determining the aromatics content of fuels in vol%.

elastomer/liquid combinations, such as elastomers in contact to automotive fuels, oils, and coolants.

$$\frac{I_{\frac{m}{z},\text{aliph}}}{I_{\frac{m}{z},\text{sum}}} = \frac{\sum_{i=1}^{9} I_{\frac{m}{z},\text{aliph,i}}}{\sum_{i=1}^{9} I_{\frac{m}{z},\text{aliph,i}} + \sum_{i=1}^{7} I_{\frac{m}{z},\text{aro,i}}} \quad (2)$$

DSC measurements to probe the glass transition temperature (T_g) were carried out in N_2 atmosphere on a DSC 204 F1 Phoenix® from Netzsch equipped with the CC300 liquid nitrogen cooler. Extracted samples of approximately 17 mg were held at −120 °C for 5 min and then heated to +100 °C at a rate of 20 °C min^{-1}. The glass transition temperature T_g was derived with the midpoint method according to Ref. [26].

Fourier-Transform Infrared spectra were acquired with a Bruker Tensor 27 on a Si-crystal of a micro attenuated total reflection (ATR) unit at room temperature. For each measurement, 32 scans in the wavenumber range 4000–400 cm^{-1} and a resolution of 4 cm^{-1} were averaged to obtain one spectrum. The spectra shown are the average of measurements at three different positions on five individual elastomer samples.

The hardness was measured with a bareiss® digi test micro Shore-A hardness testing machine according to Ref. [27]. The volume swelling was calculated from density measurements using the kit VF 4601 from Sartorius according to the Archimedes principle [5]. Tensile strength and elongation at break were determined using a Zwick testing machine with a 500 N load cell and an optical extensometer at a strain rate of 0.167 s^{-1} [23].

3. Results and discussion

3.1. Characterization of the elastomer aging

- **Oxidation of the NBR**

The aging of NBR18 samples at elevated temperatures changes the chemical composition of the elastomer, as shown by infrared spectroscopy in Fig. 2. For an exclusive focus on the aging effects of the elastomer, additives such as plasticizers were extracted before the spectra were recorded. The samples contain a high amount of carbon black (60 phr), which increasingly absorbs infrared light towards high wavenumbers. Bands at 2916/2845 cm^{-1} and 1435 cm^{-1} correspond to the stretching and deformation vibrations of CH_3 and CH_2 groups, respectively [18]. The intensity of the nitrile band at 2235 cm^{-1} is comparably weak due to the low acrylonitrile content in the NBR18 elastomer. Bands at 965 and 908 cm^{-1} are attributed to the C–H out-of-plane vibration of the C═C–H group [18]. The stretching vibration of the C═C double bond causes a band at 1640 cm^{-1} [18]. With increasing aging time and

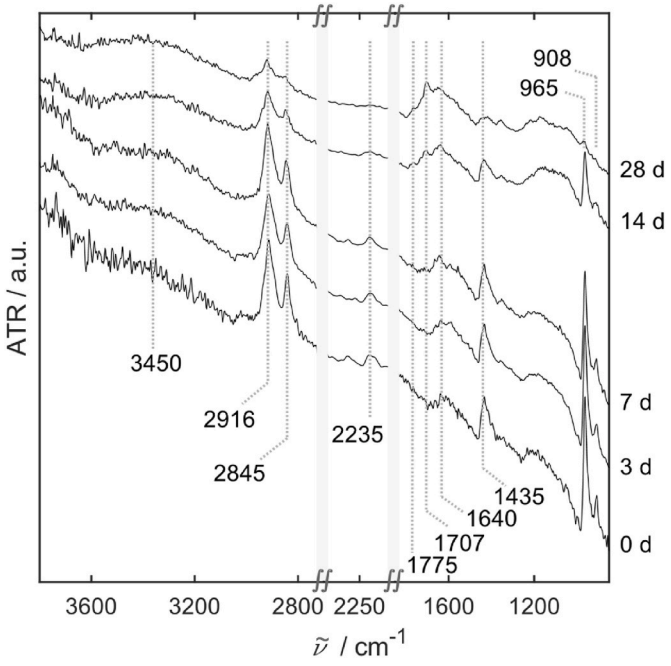

Fig. 2. ATR infrared spectra of pristine (0 d) NRB18 as well as samples aged at 120 °C up to 28 days. Spectra are shifted vertically for clarity reasons. The grey shaded spectral ranges between 2700–2300 cm^{-1} and 2200–1850 cm^{-1} are omitted for clarity.

temperature, oxidation products are formed, represented by bands at 1800–1500 cm^{-1}, originating from carbonyl groups, *e.g.*, ketones, aldehydes, esters, carboxylic acids, and carboxylates [18]. Broad bands between 3600 and 3100 cm^{-1} are attributed to OH-groups, whose intensity increases especially at high aging temperatures and correspond to oxidized species of the NBR polymer [10,18]. The upper spectrum in Fig. 2 represents a highly oxidized NBR polymer predominantly showing bands beyond 1700 cm^{-1}, which are characteristic of carbonyl groups in highly oxidized acids and esters [18]. Under these aging conditions, even the nitrile group is degraded, which is often used in other studies as a constant reference band [14,16]. For highly saturated nitrile rubbers, a possible reaction of the nitrile group by the formation of imines was suggested by Bhattacharjee et al. [28]. Moreover, the intensities of bands characteristic of the saturated C–H groups decrease. Fig. 3 (A) shows the intensity ratio of bands characteristic of oxidation products and saturated C–H-groups ($I_{1800\text{-}1700\ cm\text{-}1}/I_{2995\text{-}2760\ cm\text{-}1}$). With increasing aging time and temperature, this ratio increases, indicating a more pronounced oxidation of hydrocarbon structures under severe conditions. Fig. 3 (B) shows that the intensity ratio of bands characteristic of unsaturated and saturated hydrocarbon groups ($I_{987\text{-}887\ cm\text{-}1}/I_{2995\text{-}2760\ cm\text{-}1}$) declines with aging time and temperature, which means that unsaturated species degrade faster than saturated polymer parts by oxidation and crosslinking reactions.

- **Polymer chain mobility and degree of crosslinking**

The progressive aging of the samples is also reflected in the chain mobility and crosslink density of the elastomer. The evolution of the crosslink density was studied with swelling experiments of NBR in toluene. According to the Flory-Rehner theory [29], there is an equilibrium between the forces driving swelling, resulting from enthalpic and entropic changes due to the mixing of elastomer and solvent, and the elastic restoring force limiting swelling. Thus, in a comparative investigation (see Fig. 4), the elastomer weight fraction w_E in the swelling equilibrium is a measure of the crosslink density. w_E increases with aging time and temperature, indicating that the restoring force of

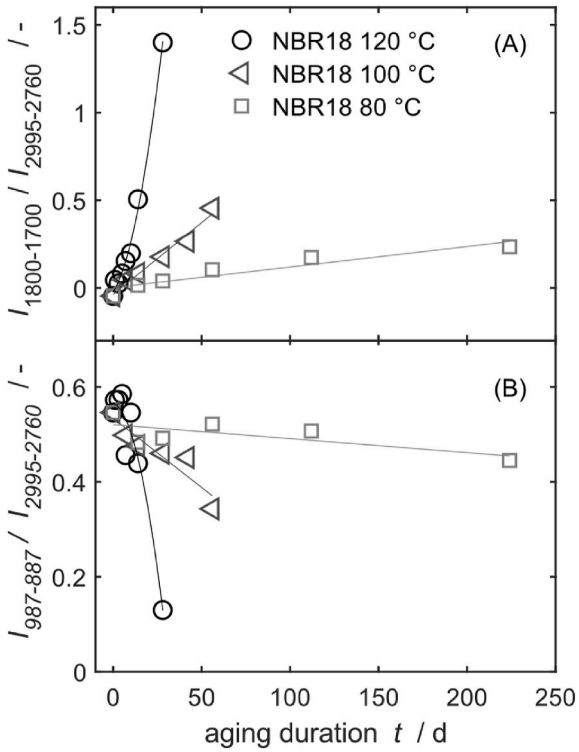

Fig. 3. (A) Intensity ratios of various oxidation products (1800–1700 cm^{-1}) and (B) of unsaturated C–H species (C═C–H out of plane vibration, 987–887 cm^{-1}) related to the saturated CH species (stretching vibration, 2995–2760 cm^{-1}).

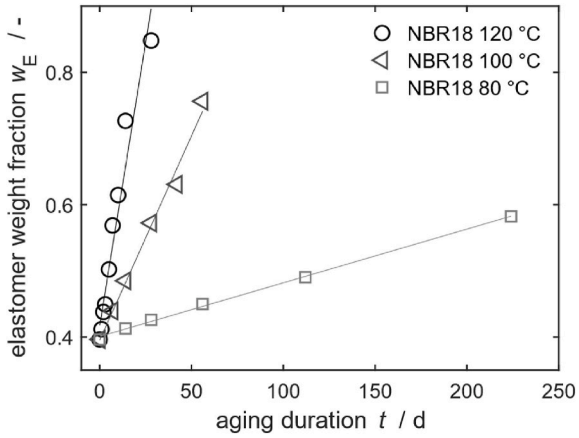

Fig. 4. Elastomer weight fraction w_E of aged NBR at swelling equilibrium in toluene as a measure for the crosslink density.

the polymer chains, and thus the crosslink density, increases. Samples with pronounced aging history, *e.g.*, 28 d at 120 °C, swell very little and behave like thermosets due to strong crosslinking. It is expected that the polymer-solvent interaction parameter changes for the aged samples, and the filler also influences the swelling behavior [30]. Therefore, w_E is not converted to the Flory-Rehner crosslink density here.

Fig. 5 shows the glass transition temperature T_g as a function of aging time and temperature. Extracted samples were used to exclude the influence of the plasticizer and to only investigate the influence of chemical changes of the elastomer by aging. The polymer chain mobility is influenced by the crosslink density, and the change in the glass transition temperature correlates with the chain mobility. Pristine NBR samples exhibit the glass transition at approximately -40 °C. The aging

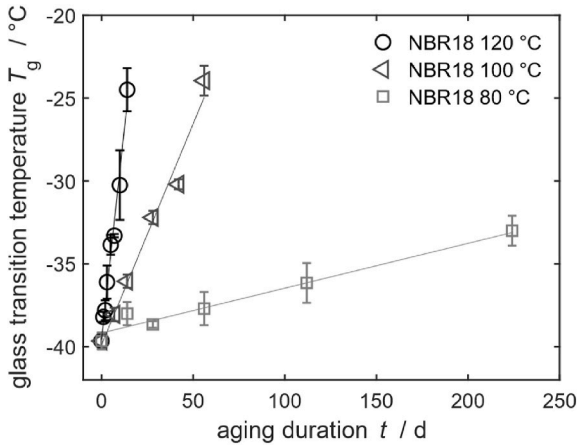

Fig. 5. Glass transition temperature of NBR after aging at different durations and temperatures.

leads to a shift of T_g to higher temperatures and indicates that the chain mobility is progressively restricted [31]. The change in T_g shows a clear temperature dependence, with higher aging temperatures causing a more rapid change. After being aged at 120 °C for 28 days, the sample does not show a clear glass transition due to its strong crosslinking.

3.2. Swelling equilibrium and sorption dynamics of model mixtures assessed by GC/MS

- **Influence of aging condition of the elastomer**

Sorption experiments are used to track the time-dependent mass uptake of model fuel components into the elastomers. At first, the model fuel mixtures 1, 2, and 3 were absorbed in elastomers that were aged at 80, 100, and 120 °C beforehand. Gravimetric experiments only yield the sorption curve of the mixture. The applied method here is an improvement compared to the gravimetric method because gas chromatography/mass spectrometry (GC/MS)-assisted sorption experiments result in the mass uptake of the individual substances separately. Exemplarily, the sorption of model mixture 2 in NBR18 at different aging conditions (A-C) and the corresponding volume fractions of model substances in the absorbed phase (a-c) are presented in Fig. 6. Volume fractions in the lower graphs were calculated by dividing the absorbed volume of each model substance by the total volume of the absorbed liquid. The volumes were calculated using the density of the individual substances and their absorbed mass depending on the sorption time. The gravimetric data show that the equilibrium mass uptakes Δm_{eq} decrease with aging time, beginning with 33.1 wt% for pristine samples and continuing with 27.1 wt% for 3 d at 120 °C and 21.5 wt% for 7 d at 120 °C. The gravimetrically determined sorption curves Δm_{grav} and the sum of absorbed model substances $\Delta m_{GC/MS}$ determined by GC/MS are in good agreement.

The diffusion coefficients, which are derived from the fit of the one-dimensional solution of Fick's second diffusion law in Eq. (1) to the gravimetrical sorption curves, also decline, which is indicated by the decreasing slope of the sorption curves. Diffusion coefficients are 8.70, 5.50 and 3.16 x 10^{-6} mm^2 s^{-1}, respectively. A detailed summary of the gravimetrically derived results is listed in Table 3. The decrease for Δm_{eq} and D, which is observed in the mixture, also applies to the individual substances mesitylene, decalin, and dodecane. With an increasing aging time of the NBR, the mass uptake at equilibrium and diffusion coefficients of all model substances decrease compared to the pristine sample (see Table 4), besides from variance in a few values. The first reason for the decrease is the aging-induced crosslinking, which increases the elastic restoring force of the polymer network. According to the free-volume theory of transport, diffusion occurs when a diffusing

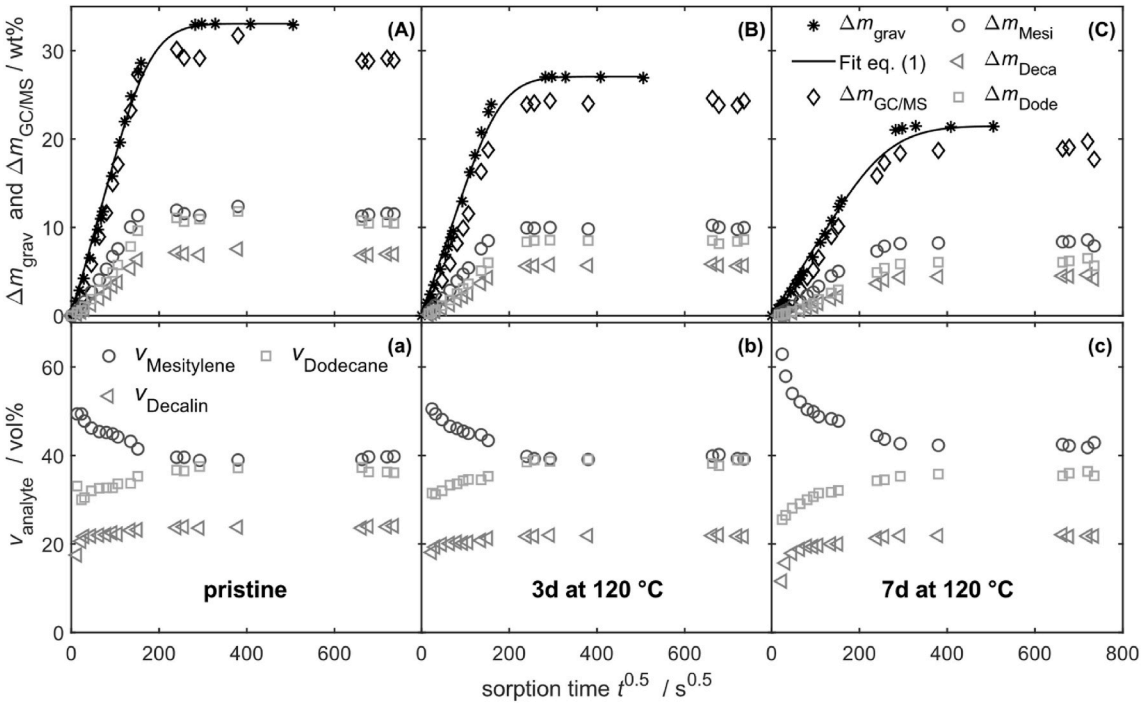

Fig. 6. Top (A–C): Sorption curves of NBR18 in model mixture 2 (mesitylene : decalin : dodecane = 20 : 20 : 60 vol%) at different aging conditions: (A): pristine, (B): 3d 120 °C, (C): 7d 120 °C, determined gravimetrically (Δm_{grav}) and by GC/MS ($\Delta m_{GC/MS}$). Bottom (a–c): corresponding volume fraction of model substances in the absorbed phase in the elastomer sample.

Table 3
Equilibrium mass uptake Δm_{eq} and average diffusion coefficients D derived by fitting Eq. (1) to the gravimetrically determined sorption curves of NBR18 in the model mixtures, respectively.

T/°C	t/d	Model mixture 1		Model mixture 2		Model mixture 3	
		$D/10^{-6}$ mm^2 s^{-1}	Δm_{eq}/wt%	$D/10^{-6}$ mm^2 s^{-1}	Δm_{eq}/wt%	$D/10^{-6}$ mm^2 s^{-1}	Δm_{eq}/wt%
80	pristine	9.68	54.9	8.70	33.1	5.79	20.6
	28	9.56	47.6	6.71	28.6	4.73	18.5
	56	8.42	44.0	6.04	26.8	4.58	17.5
	224	4.57	30.3	3.04	19.4	2.52	11.9
100	7	10.05	49.4	7.04	30.0	4.84	18.8
	14	9.90	45.4	6.45	27.9	4.20	17.3
	28	7.92	39.9	4.94	24.8	3.36	15.7
120	3	8.69	44.9	5.50	27.1	3.92	17.1
	7	5.06	33.5	3.16	21.5	2.35	13.6

molecule has enough space in the surrounding region and possesses sufficiently high energy. The specific free volume of the polymer is decreased by the crosslinking, which leads to a decreased diffusivity of penetrant molecules [32] and therefore decreased diffusion coefficients. The crosslinking in elastomers plays a major role in the swelling potential of organic liquids towards NBR, which is shown by swelling experiments of NBR where the mass uptake decreased with increasing amounts of curing agents [33,34]. The second reason is oxidation, which increases the polarity of the elastomer [28]. Decreasing equilibrium mass uptakes have also been observed in swelling experiments of NBR with increasing acrylonitrile content and thus polarity [35]. Therefore, since the polarity and crosslink density increase in the investigated samples, the uptake of the less polar model mixtures decreases.

To assess the individual affinities of the substances towards the elastomer, absolute values of the mass uptake were converted into volume fractions v by dividing the absorbed volume of one analyte by all absorbed volumes using the respective densities (see Fig. 6 a-c). According to the equilibrium values at 735 s$^{0.5}$ of the pristine sample (Fig. 6a), the aromatic mesitylene in the elastomer with $v_{mesi,el} = 40$ vol %, is enriched by a factor of 2 compared to the original composition of model mixture 2 with $v_{mesi,mix} = 20$ vol%. On the contrary, dodecane with $v_{dode,el} = 38$ vol% is depleted by a factor of 0.63 relative to the surrounding fluid with $v_{dode,mix} = 60$ vol%. Decalin is slightly enriched with $v_{deca,el} = 22$ vol% compared to $v_{deca,mix} = 20$ vol%. The strong enrichment of mesitylene originates in the interaction between its aromatic electrons and the cyano group of NBR, weakening the polymer chains' cohesive interactions [36]. The enrichment and depletion effects are enhanced with increasing aging time and temperature because more polar groups are formed in the elastomer by oxidation. Further, the specific free volume is decreased due to crosslinking. From a thermodynamic consideration, the entropy of mixing decreases when the amount of absorbed substances increases in the elastomer. Therefore, to compensate for the reduced free volume to be occupied, the uptake of mesitylene with its high affinity towards NBR is favored. The effects of aging at 120 °C on the sorption behavior can also be observed with samples aged at 100 °C and 80 °C. Longer aging times are needed to measure the same impact (see also Table 3).

To further evaluate the dynamic behavior, the volume proportions

Table 4
Equilibrium mass uptake Δm_{eq} and average diffusion coefficients D of single model mixture components derived by fitting Eq. (1) to the respective sorption curves of the individual model substances in NBR18 determined by GC/MS.

		Model mixture 1 (33.3 vol% aromatics)							
T/°C	t/d	$D/10^{-6}$ mm^2 s^{-1}				Δm_{eq}/wt%			
		Mesi	Deca	Dode	$\Delta m_{GC/MS}$	Mesi	Deca	Dode	$\Delta m_{GC/MS}$
80	pristine	8.22	6.00	4.83	6.78	25.0	16.5	9.3	50.9
	28	10.37	8.18	7.09	8.98	21.3	15.0	7.5	43.8
	56	9.66	7.22	6.71	8.21	22.7	16.2	7.9	46.7
	224	4.58	3.30	2.51	3.74	16.1	10.4	4.7	31.3
100	7	7.57	5.97	4.71	6.40	24.0	15.9	8.9	48.8
	14	7.70	6.02	4.85	6.35	23.1	14.8	8.1	46.0
	28	7.25	5.20	4.23	5.78	18.5	11.7	6.2	36.5
120	3	9.60	7.61	6.86	8.42	24.8	15.7	10.1	50.5
	7	4.63	3.62	3.25	4.02	17.4	10.6	5.4	33.4
T/°C	**t/d**	**Model mixture 2 (20 vol% aromatics)** $D/10^{-6}$ mm^2 s^{-1}				Δm_{eq}/wt%			
		Mesi	**Deca**	**Dode**	**$\Delta m_{GC/MS}$**	**Mesi**	**Deca**	**Dode**	**$\Delta m_{GC/MS}$**
80	pristine	7.27	5.23	4.72	5.74	12.4	7.5	11.8	31.7
	28	7.74	6.01	4.90	6.20	12.5	7.2	11.8	31.5
	56	5.74	4.68	3.59	4.68	11.7	6.6	10.6	28.8
	224	2.71	2.25	1.91	2.21	9.4	5.1	7.3	21.8
100	7	6.33	4.64	4.40	5.15	11.9	7.1	10.4	29.3
	14	5.03	3.70	3.40	4.09	11.2	6.5	9.5	27.2
	28	4.51	3.58	3.60	3.94	9.5	5.3	7.2	22.0
120	3	5.60	4.07	3.76	4.55	10.2	5.8	8.6	24.6
	7	2.97	2.16	2.02	2.42	8.6	4.6	6.5	19.7
T/°C	**t/d**	**Model mixture 3 (10 vol% aromatics)** $D/10^{-6}$ mm^2 s^{-1}				Δm_{eq}/wt%			
		Mesi	**Deca**	**Dode**	**$\Delta m_{GC/MS}$**	**Mesi**	**Deca**	**Dode**	**$\Delta m_{GC/MS}$**
80	pristine	5.23	3.62	3.61	4.26	4.9	2.7	10.4	18.0
	28	4.22	3.45	2.81	3.23	5.4	2.6	12.0	19.9
	56	2.92	2.62	2.08	2.31	5.2	2.4	11.0	18.7
	224	2.16	2.09	1.56	1.80	4.1	1.8	7.6	13.5
100	7	4.07	3.00	3.24	3.43	5.4	2.8	10.6	18.6
	14	3.68	2.69	1.26	1.31	4.9	2.4	9.1	16.4
	28	1.87	1.87	1.39	1.50	4.6	2.4	8.8	15.8
120	3	2.78	2.23	2.18	2.63	5.4	2.7	11.7	19.8
	7	2.37	1.62	1.86	1.96	3.9	2.0	6.6	12.5

Abbreviations: Mesi: Mesitylene; Deca: Decalin; Dode: Dodecane.

are compared in dependency on the sorption time. At the beginning of the sorption experiment, an interesting phenomenon is discovered. The mesitylene proportion is even more enriched with $\nu_{mesi,el} = 50$ vol% compared to the equilibrium at 735 s$^{0.5}$ with $\nu_{mesi,el} = 40$ vol%. Due to the high affinity of aromatic compounds towards NBR, the diffusion of mesitylene into the elastomer is faster. Therefore, the aromatic compounds cause the swelling predominantly at the beginning of the experiment. When the elastomer is swollen partially, the affinity for all substances towards NBR equalizes, and the diffusion is promoted for decalin and dodecane. The interaction of mesitylene with the cyano groups lowers the resulting polarity of the elastomer. Further, the increasing amounts of nonpolar mesitylene, decalin, and dodecane create an increasingly less polar environment in the elastomer and promote the uptake of dodecane and decalin. With increasing amounts of decalin and dodecane, their relative fractions increase in the elastomer, and the relative fractions of mesitylene decrease until the equilibrium is reached. The preferred uptake of the mesitylene at the beginning of the sorption experiment becomes even more pronounced with increasing aging time and temperature due to polar groups being formed during oxidation.

- **Influence of aromatics content**

To study the influence of the aromatics content on the sorption behavior, the aromatics content was varied between 10 vol% to 33.3 vol % in the model fuel mixtures 3 to 1. Fig. 7 shows the sorption of this model fuel mixtures and its corresponding volume fractions after immersion of the NBR, which was aged for 3 d at 120 °C beforehand. The aromatics content of the immersing fluid declines in the order of the model mixtures 1, 2, and 3 and correlates with the reduction of the equilibrium mass uptakes (see Fig. 7 A > B > C) as well as the diffusion coefficients. The total mass uptakes are 44.9 wt%, 27.1 wt%, and 17.1 wt% for the model mixtures 1 to 3. The diffusion coefficients, as represented by the initial slope of the gravimetrically determined sorption curves, are 8.69, 5.50 and 3.92 x 10^{-6} mm^2 s^{-1} (for an overview see also Table 3). In Fig. 7(a–c) the volume fractions are shown and the aromatic mesitylene is enriched again. However, the enrichment of the aromatic mesitylene is more evident when the aromatic fraction is low. This is shown by the relative volume fractions at equilibrium relative to the immersion liquid, as shown in Fig. 7 a-c: 48 vol%/33.3 vol% = 1.45 (mix 1); 40 vol%/20 vol% = 2 (mix 2); 25 vol%/10 vol% = 2.5 (mix 3). The enrichment and depletion in dependency on mixture composition as well as aging time and temperature are summed up in Fig. 8 (A-C). Enrichment and depletion factors are introduced here to describe the affinity of the single substances towards the elastomer. A factor of >1 indicates an enrichment, a factor <1 shows depletion, and a factor = 1 means equal concentrations of a substance in the elastomer at swelling equilibrium compared to the concentration in the immersion liquid.

Mesitylene (A) is constantly enriched (factor >1) compared to the immersion liquid due to its high affinity towards NBR18. When the

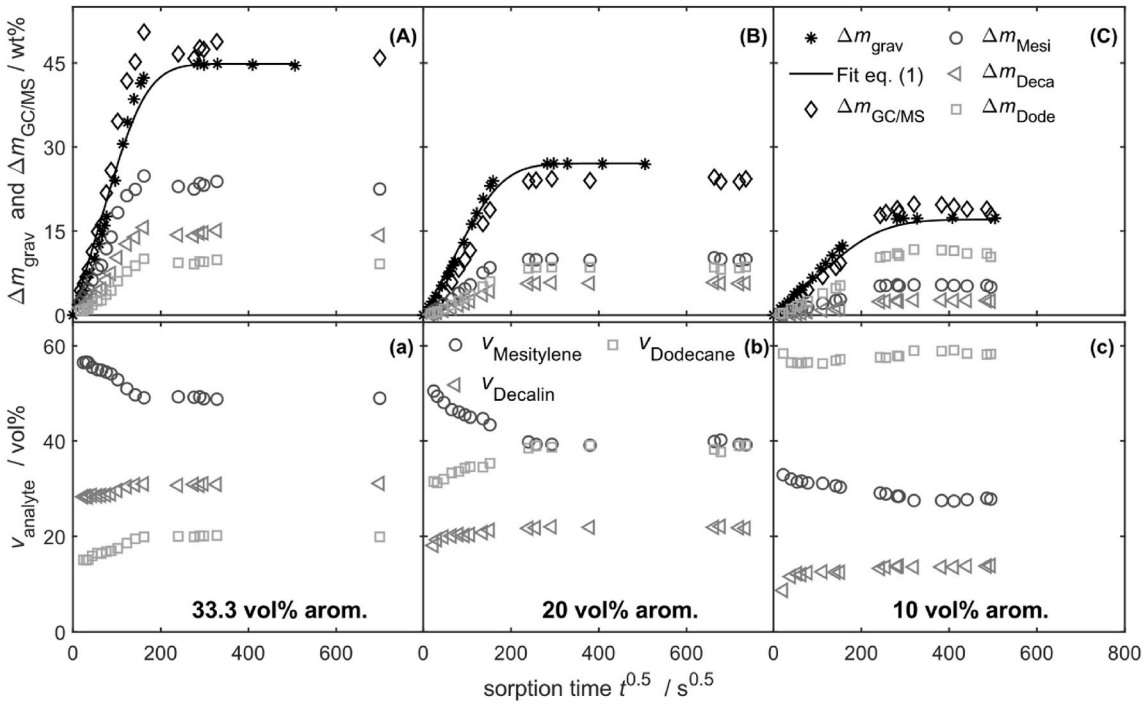

Fig. 7. Top (A–C): Sorption curves of NBR18 after aging for 3 d at 120 °C in different model fuel mixtures: (A): model mixture 1, (B): model mixture 2, (C): model mixture 3, determined gravimetrically (Δm_{grav}) and by GC/MS ($\Delta m_{GC/MS}$). Bottom (a–c): corresponding volume fraction of model substances in the absorbed phase in the elastomer sample.

aromatics content of the immersion liquid decreases, like in the order of model mixture 1 to mixture 3, the relative enrichment of mesitylene increases. For pristine samples with decreasing aromatics content, the enrichment factors for mesitylene are 1.45, 1.85, and 2.54. After being aged for 7 d at 120 °C, the corresponding enrichment factors are 1.55, 2.1, and 2.95. Thus, the enrichment factors for the aromatic mesitylene increase when the aromatics content of the immersing liquid decreases or when the samples are aged for longer aging durations. Lower aging temperatures also lead to an enrichment of mesitylene, but longer aging durations must be applied to obtain the same increase of the enrichment factors. Contrary, dodecane (C) with a low affinity to the elastomer is always depleted (factor <1) compared to the immersion mixture, especially when the initial concentration in the immersion liquid (model mixture 1) is low. Decalin (B) with a medium affinity is depleted compared to the mixture when the fraction of decalin and aromatic mesitylene in the mixture is high (mixture 1). Decalin is slightly enriched when the initial concentration is low (model mixture 3) and a compound with low affinity like dodecane dominates the mass uptake. Overall, decalin changes from depletion to enrichment, and no clear influence of the aging temperature is visible. Details of Δm_{eq} and D in dependency on the aging time and temperature for the individual substances are listed in Table 4. The equilibrium mass uptake Δm_{eq}, as well as D, decreases for mixtures with decreasing aromatics content and for the individual substances when the aging time and temperature are increased. These results are used to calculate activation energies for elastomer aging in the following.

3.3. Activation energy of D and Δm_{eq} as a measure for the aging

The influence of the aging temperature on the sorption behavior is additionally assessed by evaluating activation energies. Often, sorption experiments of pristine samples are carried out at different temperatures. The activation energy, in that case, is a measure of the temperature dependency of the diffusion processes [37]. However, the change in the diffusion coefficients D and the equilibrium swelling degree Δm_{eq} is also dependent on the elastomers aging temperature and history prior to the sorption. Sorption experiments, all carried out at room temperature, can be used to determine the activation energy characteristic of the elastomer aging. The activation energies are determined by Arrhenius plots using the parameters D and Δm_{eq} in dependency on the temperatures of the elastomer aging (see Table 3). To compare the activation energies with other methods, also the evolution of the elastomer oxidation and consumption of the double bond from IR spectra (Fig. 3), the elastomer weight fraction w_E from toluene swelling (Fig. 4), and the glass transition temperature T_g (Fig. 5) are evaluated. The curves in dependency on the aging time are assessed according to the Time-Temperature-Superposition principle (TTS) [19]. The reference temperature $T_{ref} = 100$ °C is used to calculate the master curves. The abscissae of the experimental data, determined at 120 °C and 80 °C, are multiplied by shift factors a_T for the aging time to match the master curve best (Fig. 9). The Arrhenius plot with the logarithmic shift factors ln a_T versus $1/T$ is shown in Fig. 10, and the respective activation energies are listed in Table 5. The activation energy is assessed using Eq. (3), with the universal gas constant R = 8.314 J/K mol [19].

$$\ln(a_T) = \frac{E_a}{R} \cdot \left(\frac{1}{T_{ref}} - \frac{1}{T} \right) \quad (3)$$

The values for E_a, determined with equilibrium swelling and diffusion coefficients, for the stabilized elastomers in this study vary between 91–102 kJ/mol (Table 5). The values are in good agreement with reported values (74.3–112.4 kJ/mol) in the literature [12,38,39], using compression set, oxygen consumption, elongation at break, and swelling. The activation energies in this study, determined for the aging dependent change in w_E and T_g, are 93 kJ/mol and 103 kJ/mol, respectively, and lie within the same range as values determined for diffusion and equilibrium swelling. Buckley et al. [12] determined activation energies for the change in crosslinking of NBR aged in JP5, Camelina, and dodecane. This approach is like the change in Δm_{eq}, without Δm_{eq} being converted to a crosslink density employing the Flory-Rehner theory. To our best knowledge, the determination of activation energy for an underlying aging process through the change in diffusion coefficients is new and thus an extension of the methods to

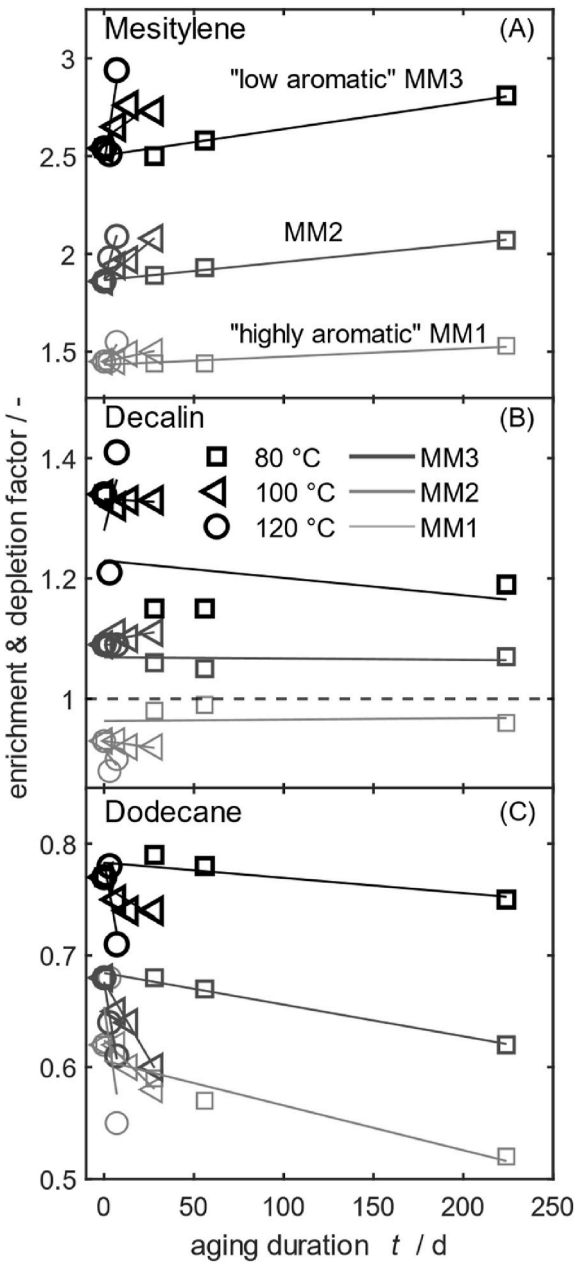

Fig. 8. Enrichment and depletion factors of model substances in the absorbed liquid in the elastomer related to the immersion liquid for mesitylene (A), decalin (B) and dodecane (C). Each diagram shows the factors for all three model mixtures (MM1, MM2, MM3), the aging temperatures of 80, 100, and 120 °C in dependency on the aging time.

determine activation energies of aging processes. Recently, Pazur et al. published a comprehensive experimental work to evaluate the activation energies of carbon black filled, stabilized NBR with different acrylonitrile content determined by various experimental techniques (75–93 kJ/mol) [19] like Micro Shore A hardness, tensile strength, and swelling. Further, infrared spectroscopy was applied to extract activation energies of 76–81 kJ/mol for unstabilized and unfilled NBR [18]. The present study extends IR determined activation energies for stabilized and filled NBR18 elastomers. The activation energies are 88 kJ/mol for the evolution of oxidation products (IR_{Oxi}, Table 5) and 78 kJ/mol for the loss of unsaturation (IR_{DBB}, Table 5). The activation energies E_a for D and Δm_{eq} for the model mixtures 1–3 are similar. No significant differences are observed within statistical errors, even though for higher contents of aromatics (model mixture 1), lower activation energies are expected.

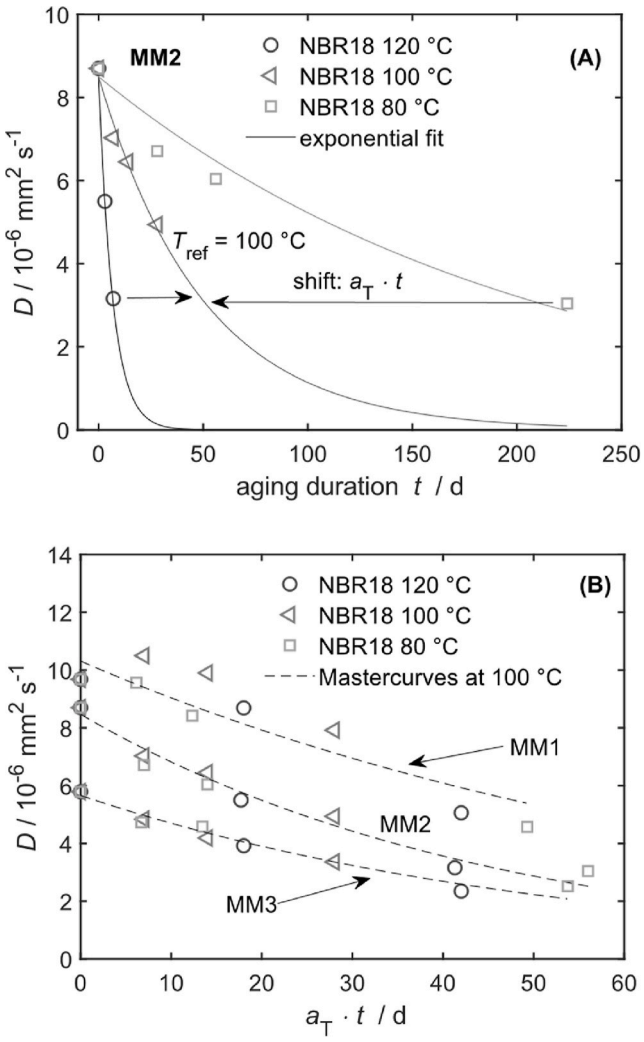

Fig. 9. Diffusion coefficients D of model mixture 2 in aged NBR specimens in dependency on the aging time (A). The master curve is obtained by multiplying the aging time t with the shift factors a_T to achieve the best matching curve. Master curves for the three model mixtures (B).

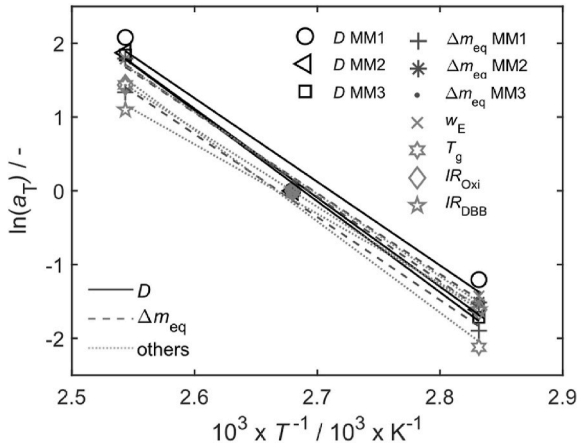

Fig. 10. Arrhenius plot of ln a_T of D and Δm_{eq} for the model mixtures MM1-3 as well as from w_E, T_g, and IR data versus the reciprocal aging temperature. The activation energy E_a is extracted from the slope using Eq. (3).

Table 5
Activation energies in kJ/mol are given for the aging processes determined with the diffusion coefficients D and equilibrium mass uptakes Δm_{eq} for model mixtures 1–3 and toluene (elastomer weight fraction w_E). Additionally, corresponding values are given for the glass transition temperature T_g, the evolution of oxidation (IR_{Oxi}), and consumption of the double bond (IR_{DBB}).

	Toluene		MM1		MM2		MM3	
	E_a	R^2	E_a	R^2	E_a	R^2	E_a	R^2
D			94 ± 11[a]	0.967	100 ± 5[a]	0.995	102 ± 3[a]	0.997
Δm_{eq}	93 ± 6[a]	0.991	94 ± 4[a]	0.995	95 ± 5[a]	0.994	91 ± 6[a]	0.989
T_g	103 ± 5[a]	0.994						
IR_{Oxi}	88 ± 1[a]	0.999						
IR_{DBB}	78 ± 4[a]	0.994						

[a] The uncertainties in the activation energies were calculated based on t-statistics with a confidence interval of 68% for the slope in the Arrhenius plot.

The differences in the activation energies obtained from infrared spectroscopy compared to the other methods are attributed to diffusion-limited oxidation profiles throughout the samples [16]. ATR Infrared spectroscopy is a surface-sensitive method and thus less prone to aging gradients in the bulk when the measurement is conducted on the surface. The effect of the aging temperature on properties like the diffusion coefficient, equilibrium swelling, and glass transition temperature is stronger since the parameters are more sensitive to aging induced crosslinking and polarity profiles, representing more the bulk of the elastomer.

3.4. Swelling and sorption dynamics of real fuels assisted by GC/MS

After investigating the sorption behavior with pre-extracted specimens, this section focuses on additive-containing specimens in contact with complex real fuels. The insights from the experiments with model mixtures, gained in chapter 3.2, are used here to support the interpretation of the behavior of real fuels. The real fuels are compared to the model mixtures, especially MM2, with a similar aromatics content of 20 vol%. To evaluate the influence of the fluid on mechanical properties, testing of NBR18 dumbbell specimens with fuel contact is performed. In Fig. 11 (A) the gravimetrically determined mass uptakes Δm_{grav} of the NBR18 samples after the immersion in ReadiJet and Jet A-1 is shown. It is apparent, that the elastomer gains weight with proceeding sorption time. For aged samples, the equilibrium mass uptakes Δm_{eq} are lower than those for the pristine samples. The mass uptake at equilibrium for the pristine elastomer in ReadiJet is 19.0 wt% and decreases to 13.4 wt% when the elastomer was aged 7 d at 120 °C before (see Table 6). The mass uptakes also decrease when the aromatics content of the surrounding liquid is reduced since neat ReadiJet contains 21.2 vol% and Jet A-1 contains 16.2 vol% aromatics. The mass uptake of the unaged elastomer with ReadiJet is 19.0 wt%, whereas it is 15.5 wt% for Jet A-1. The reduction in the mass uptake with longer aging times and lower aromatics contents is also described in chapter 3.2 when NBR18 is immersed in model mixtures. The mass uptakes Δm_{eq} in this experiment (see Fig. 11 (A)) are lower than those of model mixture 2 with an aromatics content of 20 vol% in chapter 3.2 (for Δm_{eq}, see Fig. 6/Table 3: pristine: 33.1 wt%; 3 d 120 °C: 27.1 wt%, 7 d 120 °C: 21.5 wt%).

Since the elastomers in this part of the study contain soluble additives, which are extractable by the fuel, the mass uptake is convoluted with the loss of additives. The concentration of soluble components in dependency on the sorption time is investigated with the assistance of GC/MS analysis as it is shown in Fig. 11 (B). For reasons of simplicity, only the soluble fractions from the experiments with ReadiJet are displayed. Firstly, the intercept at the ordinate is attributed to the additive fraction in the unswollen elastomer. This value displays the influence of aging. With longer aging times, the plasticizer DEHP desorbs thermally from the elastomer, and the antioxidant 6PPD is consumed. Thus, their amount is reduced for aged samples. Secondly, the overall mass uptake m_t, determined by weighing (see Fig. 11 (A)), is here corrected for the loss of additives to yield only the uptake of ReadiJet according to Eq. (4).

$$\begin{aligned} m_0 &= m_{elast+add,0} \cdot \left(1 - w_{DEHP,0} - w_{6PPD,0}\right) \\ m_{solubles,t} &= m_t - m_0 = m_{fuel,t} + m_{DEHP,t} + m_{6PPD,t} \\ \Delta m_{fuel,t} &= \left(m_{solubles,t} - m_{DEHP,t} - m_{6PPD,t}\right) / \, m_0 \cdot 100\ \% \end{aligned} \tag{4}$$

The concentrations of DEHP and 6PPD (w_{DEHP}, w_{6PPD}) are known from the GC/MS analysis, and the overall mass change is known from weighing for every point of sorption time. The initial amount of the additives at $t^{0.5} = 0\ s^{0.5}$ is subtracted from the elastomer weight prior to the immersion $m_{elast\ +\ add,0}$ to get the elastomer weight m_0 not containing any soluble components [25,40]. Further, the mass of solubles $m_{solubles,t}$ is the sum of the additive masses ($m_{DEHP,t}$, $m_{6PPD,t}$) and the absorbed fuel at time t ($m_{fuel,t}$). The mass change due to absorption and extraction processes can thus be separated to only yield the mass uptake of the fuel components $\Delta m_{fuel,t}$, which is denoted as $\Delta m_{eq,uptake}$ in the equilibrium. The equilibrium mass uptake $\Delta m_{eq,uptake}$ in ReadiJet again decreases with longer aging times and lies at 36.4 wt% for pristine and 22.4 wt% for the NBR18 aged 7d at 120 °C (see Table 6). In comparison, the absorbed amount of ReadiJet is higher than that of Jet A-1. 36.4 wt% ReadiJet and 32.5 wt% Jet A-1 are absorbed for pristine samples. The reason for that is a lower content of aromatics in Jet A-1 (16.2 vol% instead of 21.2 vol%). The mass uptake of model mixture 2 is 34.9 wt% and is similar to the values of the real fuels. In chapter 3.2, the mass uptake of model mixture 2 (here $\Delta m_{eq} = \Delta m_{eq,uptake}$), which is investigated after extraction of the soluble additives, is determined to be 33.1 wt%. Therefore, the corrected mass uptakes are valid because of only marginal differences. The time-dependent sorption behavior is characterized by diffusion coefficients of the fuel uptake process D_{uptake}, summarized in Table 6. The diffusion coefficients D_{uptake} for ReadiJet are 14.3 x 10^{-6} $mm^2\ s^{-1}$ for the pristine, 6.5 x 10^{-6} $mm^2\ s^{-1}$ for 3 d at 120 °C, and 2.8 x 10^{-6} $mm^2\ s^{-1}$ for samples aged for 7 d at 120 °C. The diffusion coefficients are higher than that of Jet A-1 and lower than that of the model mixture 2. A cause for that is a higher amount of aromatics in ReadiJet compared to Jet A-1. Additionally, the diffusion coefficient of model mixture 2 is comparably high because the average molecular size of the constituents in model mixture 2 is smaller than that of the constituents in ReadiJet or Jet A-1. Since smaller molecules diffuse faster, they consequently exhibit higher diffusion coefficients. In chapter 3.2, Table 3, the diffusion coefficients D for model mixture 2 and pre-extracted elastomers are listed (8.70, 5.50, 3.16 x 10^{-6} $m^2\ s^{-1}$). They are significantly lower than D_{uptake} of additive-containing specimens at an identical aging temperature of 120 °C and durations of 3 and 7 days. The cause is that additives swell the elastomer, and therefore the mobility of the polymer chains is increased, which enables higher diffusivity for penetrant molecules. Furthermore, the additives are less polar than the cyano groups in NBR, which improves the compatibility to the mainly nonpolar fuel components.

As depicted in Fig. 11 (C) for the aromatics, the composition of the absorbed fuel is analyzed regarding its hydrocarbon types in dependency on the sorption time. At the beginning of the sorption experiment the amount of absorbed aromatics is high due to their high affinity towards NBR [36], as already described in chapter 3.2. With increasing sorption time, substances with slower diffusion kinetics, such as alkanes

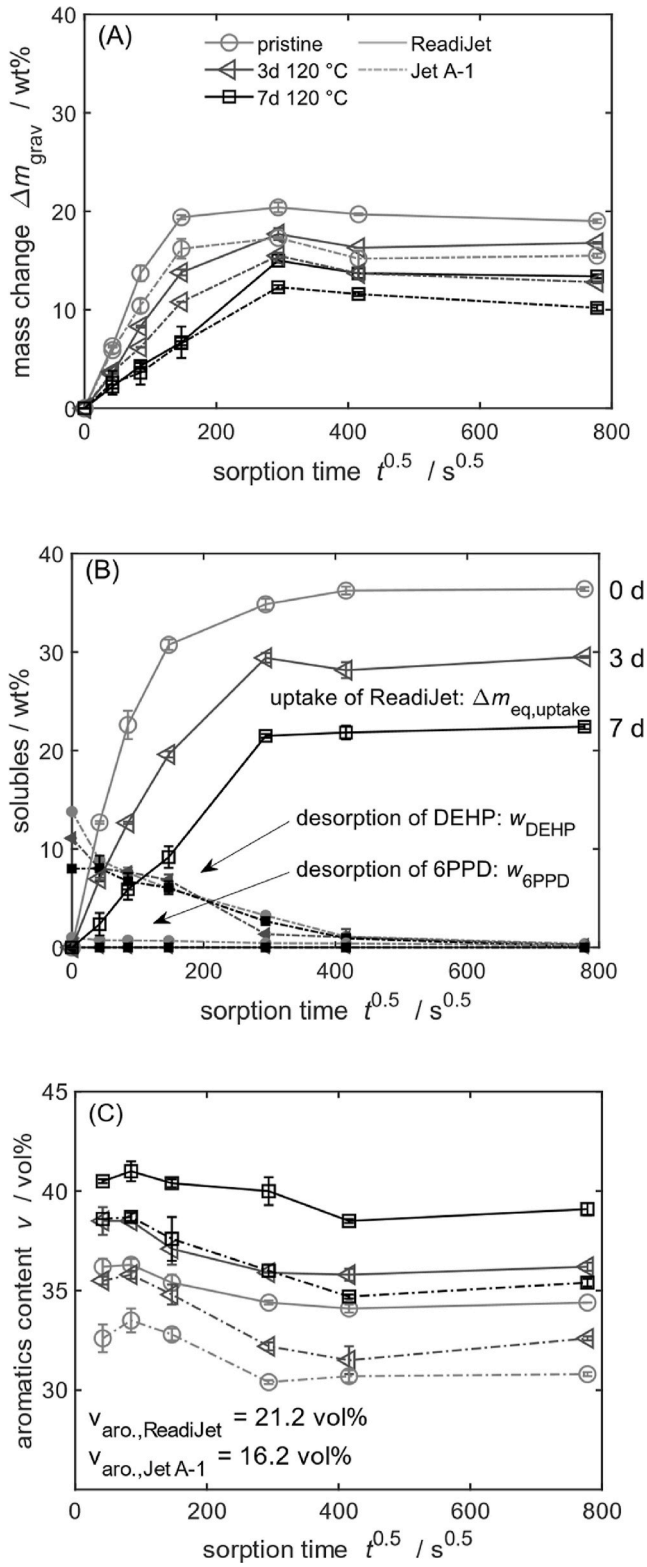

Fig. 11. Mass change Δm_{grav} of NBR18 after immersion in ReadiJet (solid line) and Jet A-1 (dotted line) (A). Uptake of ReadiJet into NBR18 and simultaneous desorption of DEHP and 6PPD by GC/MS (B). Aromatics content in the absorbed liquid phase in the elastomer (C). Samples were aged at 120 °C for 7 days (□), 3 days (◁), or pristine (○).

Table 6
Overview of different parameters obtained from NBR18, pristine and aged at 120 °C. Parameters are obtained in the swelling equilibrium ($t^{0.5}$ = 778 $s^{0.5}$) after immersion in model mixture 2 (MM2), Jet A1, and ReadiJet.

t_{aging}/d	MM2	Jet A-1	ReadiJet	t_{aging}/d	MM2	Jet A-1	ReadiJet
	Δm_{eq}/wt%				**Micro Shore A hardness/-**		
pristine	17.4	15.5	19.0	pristine	60.3	63.4	61.0
3	14.8	12.8	16.8	3	67.7	70.5	67.9
7	11.5	10.2	13.4	7	77.9	83.0	83.7
	$\Delta m_{eq,uptake}$/wt%				**ρ/g cm^{-3}**		
pristine	34.9	32.5	36.4	pristine	1.070	1.081	1.074
3	27.5	23.9	29.5	3	1.093	1.107	1.096
7	20.4	18.9	22.4	7	1.127	1.147	1.141
	$D_{uptake}/10^{-6}$ mm^2 s^{-1}				**ε_B/%**		
pristine	17.4	11.9	14.3	pristine	130	192	181
3	15.0	5.7	6.5	3	84	81	101
7	7.7	3.5	2.8	7	57	39	34
	Enrichment factors				**σ_B/MPa**		
pristine	2.0	1.9	1.6	pristine	7.7	11.1	7.7
3	2.1	2.0	1.7	3	8.2	7.2	8.2
7	2.2	2.2	1.8	7	10.3	8.9	10.3

or cycloalkanes, also diffuse into the elastomer, which leads to a relative reduction of the amount of aromatics. The enrichment factors for aromatics in the swelling equilibrium are quite similar for the fuels. According to Table 6, in the pristine elastomer, they are 1.6 for ReadiJet, 1.9 for Jet A-1, and 2.0 for model mixture 2, respectively. For the aged samples they increase to 1.7, 2.0 and 2.1 for 3 d at 120 °C and 1.8, 2.2 and 2.2 for 7 d at 120 °C. The aromatics content in the swollen elastomer at equilibrium is slightly lower in the synthetic fuel ReadiJet than in the model mixture, *e.g.*, for pristine samples, 34.4 vol% (ReadiJet) vs. 39.8 vol% (MM2, see Fig. 6a), even if the aromatics content in neat ReadiJet is higher than in MM2. Hence, the swelling behavior can not only be explained by the aromatics content. In the model mixture, branched and sterically demanding substances are not represented, but they are part of ReadiJet and Jet A-1, which may explain the deviation. ReadiJet consists of n-alkanes (C_8 to C_{16}), alkyl-substituted cyclohexanes and cyclopentanes, alkylbenzenes (C_3 to C_8), indanes, tetrahydronaphtalenes and its derivatives [20]. The fossil fuel Jet A-1 consists of a similar composition [20] but a lower aromatics content in this case. It is reported [25], that the aromatic *m*-xylene possesses a high diffusion coefficient and a relatively high swelling potential for NBR. Naphtalenes otherwise exhibit high swelling potentials and relatively low diffusion coefficients, whereas *iso*-hexadecane has a low diffusion coefficient and low swelling potential. Overall, the model mixtures simulate the investigated fuels well regarding their diffusion properties, but not perfectly due to the deviating composition of complex real fuels.

3.5. Mechanical testing of aged NBR swollen in real fuels

The physical and mechanical testing results of the elastomers in dependency on the sorption time $t^{0.5}$ and aging time at 120 °C are summarized in Fig. 12 and Table 6. The density measurements and the calculated volume change (see Fig. 12 (A)) are, for the sake of clarity, only depicted for ReadiJet. The Micro Shore-A hardness (Fig. 12 (B)), the elongation at break (C), and stress at break (D) are shown for ReadiJet and Jet A-1 in comparison. The initial values at $t^{0.5}$ = 0 $s^{0.5}$ represent the properties of the aged elastomers before the fuel contact. With increasing aging time, the density (A) and the Micro Shore-A hardness (B) increase, whereas the elongation at break (C) and strain at break (D) decrease. This confirms the additional crosslinking of the elastomer due to the aging [41]. The initial increase in the density (A, left axis) from 1.160 g cm^{-3} (pristine) to 1.200 g cm^{-3} (3d 120 °C) and to 1.225 g cm^{-3} (7d 120 °C) is attributed to the shrinking of the elastomer during aging. The shrinking is caused by the additives, mainly DEHP, which evaporates because of the elevated temperatures during aging. A second factor is that oxygen is bound to the elastomer by

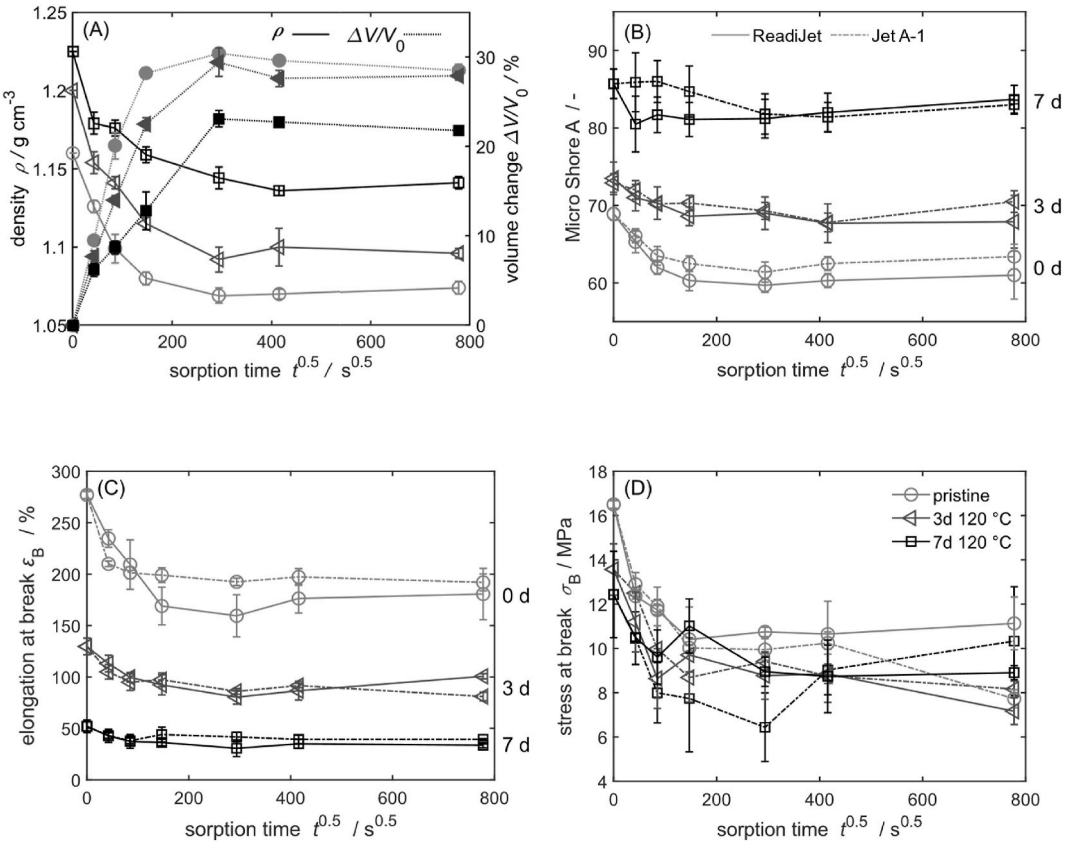

Fig. 12. Density (left axis, unfilled markers) and the calculated volume change (right axis, filled markers) for ReadiJet; Jet A-1 is not shown. (A), Micro Shore-A hardness (B), elongation at break (C), and stress at break (D) of the elastomer in dependency on the sorption time. Samples were aged at 120 °C for 7 days (□), 3 days (◁), or pristine (○).

oxidation reactions, as observed by IR spectroscopy, increasing the elastomer mass. The density decreases with more fuel being absorbed into the specimen. NBR18, model mixure 2, Jet A-1 and ReadiJet have densities of 1.160 g cm^{-3}, 0.802 g cm^{-3}, 0.812 g cm^{-3}, and 0.823 g cm^{-3}, respectively, and the resulting equilibrium density lies between these values. From the density and the mass change, the volume change (A, right axis) can be calculated, which is only displayed for ReadiJet and not corrected for the extraction of additives. The elastomer swells by 28.5 vol% relative to the initial volume V_0 for pristine and 21.8 vol% for the aged sample (7 d at 120 °C). According to Table 6, the densities of all investigated swollen elastomers are similar in the equilibrium. Due to aging, the elastomer gets harder, which is reflected in the initial hardness values of 68.9, 73.5, and 85.7 Micro Shore-A. The elastomer softens with proceeding sorption time, which is shown by a drop in Micro Shore-A hardness (B). The curve progression of the hardness values is similar for Jet A-1 and ReadiJet. Overall, the softening effect, caused by the uptake of fuel, is more pronounced than the hardening effect due to the extraction of plasticizer. After about 6 h (147 s$^{0.5}$), equilibrium hardness is reached below the initial value. The drop in the hardness appears faster, and the final hardness is lower for ReadiJet than Jet A-1, which is attributed to its higher aromatics uptake. For the aged samples, the relative change in hardness is smaller than for the pristine sample, because less fuel is absorbed, less plasticizer is extracted, and the elastomer is stiffer generally.

The elongation at break (C) decreases with longer aging times for the pristine, unswollen elastomer from 277% to 130% and 52% (3 d and 7 d 120 °C). With further crosslinking, more chemical bonds are formed between the macromolecules. Consequently, the elongation is more restricted, and shorter elongations occur, until the polymer chains are fully stretched and break. Regarding the swollen elastomer, the polymer chains are already pre-stretched due to the liquid uptake and volume increase. This results in shorter possible elongations in comparison to the unswollen state and the decrease in the elongation at break ε_B is less pronounced for Jet A1 than for ReadiJet as in the equilibrium, the elongations at break of the pristine samples are 192% and 181%, respectively. The pristine NBR18 exhibits an ε_B of 130% in model mixture 2 in the equilibrium. The difference of ε_B for samples aged for 7 d at 120 °C is only marginal in both fuels and MM2. This is attributed to the fact that these samples are strongly crosslinked, and the fuel uptake is low. However, the aging effects dominate the elongation at break. The stress at break (D) decreases with longer aging durations from 16.5 MPa to 13.6 MPa and 12.4 MPa. When subsequently fuel is absorbed, there is a further reduction in the stress at break, possibly because the polymer-polymer, polymer-filler, and filler-filler interactions are weakened due to the liquid uptake. Due to the swelling, a pre-stress is present, and therefore samples break at lower stress and elongations compared to the unswollen samples [42].

Overall, this work covers different stages of the life of an elastomer. It covers pristine material with undegraded properties, severely aged samples (*e.g.,* 7 d at 120 °C) which are no longer usable, and samples with moderate aging (*e.g.,* 3 d at 120 °C). Since the whole range of aging degrees is considered, predictions about the service life can be made in dependency on respective material specifications. In summary, the chemical changes and the physical and mechanical responses of the pristine and aged NBR18 to ReadiJet and Jet A-1 are similar due to the comparable chemical composition of the fuels. Investigations with simplified model mixtures explain and assist the interpretation of the characteristics of real fuels. Furthermore, the model mixtures composed of mesitylene, decalin and dodecane show a good estimate of the swelling behavior of NBR18 in ReadiJet and Jet A-1. The results points in the direction that ReadiJet and Jet A-1 behave similarly in the long term. To manifest this statement, more investigations on the swelling

behavior of aged elastomers in synthetic fuels should be the object of future research.

4. Conclusion

This study presents a comprehensive investigation of the sorption dynamics and swelling behavior of aged acrylonitrile-butadiene rubbers (NBR) in contact with fuels combined with mechanical testing. To simulate elastomers in seals, hoses, and tank linings after long service periods, the focus is laid on pre-aged elastomers.

Aged samples are characterized by IR spectroscopy, DSC, and swelling in toluene to quantify increasing oxidation, decreased mobility of polymer chains, and additional crosslinking of the elastomers. The activation energies of elastomer aging are determined by time-temperature superposition using the change in diffusion coefficients of model mixtures in elastomers at different aging temperatures to be in the range of 91–102 kJ/mol.

Based on model substance mixtures, general concepts of fuel diffusion are evaluated in-depth using gravimetric and GC/MS-assisted sorption experiments. In this way, considering fuel diffusion, composition- and structure-to-property relationships of aged NBR are better understood. Corresponding findings from simple model mixtures are transferable to the synthetic aviation fuel ReadiJet and the conventional kerosene Jet A-1.

It is found that the equilibrium mass uptakes of NBR18 and the diffusion coefficients depend on the fuel composition and the degree of aging of the elastomer. GC/MS analysis shows that the composition of the absorbed model substances or fuels in the elastomer differs from that in the immersion liquid as aromatics are enriched in the elastomer and (cyclo)alkanes are depleted. This is attributed to interactions between the cyano group in the NBR and the fuel constituents. Aromatics preferably interact with the cyano group and reduce its polar character. Therefore, they are mainly absorbed into the elastomer. The affinities between the surrounding fuel and the elastomer equalize with longer sorption times, and the uptake of nonpolar substances such as alkanes is promoted. Higher concentrations of aromatics are found in aged elastomers compared to pristine elastomers, explained by the increased polarity of the elastomer due to oxidation and additional crosslinking.

Significant differences in diffusion processes are observed whether the elastomer was extracted before immersion in the fuel or not. The presence of plasticizers and other extractable components in the elastomer in general accelerate exchanging processes and the uptake of fuel components. However, a quantitative characterization of a component selective diffusion requires comprehensive chemical analyses. For a precise characterization of in-service elastomer components, for example GC/MS, are inevitable.

Model mixtures show good predictions of the fuel properties but are less complex in their composition than real fuels to explain details. Aging effects and their impact on mechanics and swelling are quantifiable, allowing the estimation of potential failure. Better knowledge of failure conditions promotes the sustainable and safe use of elastomers in contact with fuels. This study shows that the physical and mechanical responses of pristine and aged NBR specimens in contact with ReadiJet and Jet A-1 are similar in the long term.

Funding

We acknowledge the financial support by FORscience Research Fund of the Universität der Bundeswehr München for open access publication.

Declarations

The authors declare that they have no known competing financial interests or personal relationships that could have appeared to influence the work reported in this paper.

Data availability

The raw/processed data required to reproduce these findings cannot be shared at this time due to legal or ethical reasons.

Author statement

Benedikt Demmel: Writing - Original Draft, Investigation, Tobias Förster, Writing - Review & Editing, Project administration, Funding acquisition, Supervision, Sebastian Eibl, Writing - Review & Editing, Supervision, All authors have read and agreed to the published version of the manuscript.

Declaration of competing interest

The authors declare that they have no known competing financial interests or personal relationships that could have appeared to influence the work reported in this paper.

Acknowledgment

The support of Prof. Dr. Alexander Lion and Prof. Dr. Michael Johlitz from the Universität der Bundeswehr München, Fakultät für Luft-und Raumfahrttechnik, Institut für Mechanik is gratefully acknowledged.

References

[1] W. Wang, L. Tao, Bio-jet fuel conversion technologies, Renew. Sustain. Energy Rev. 53 (2016) 801–822, https://doi.org/10.1016/j.rser.2015.09.016.
[2] Y. Bicer, I. Dincer, A comparative life cycle assessment of alternative aviation fuels, Int. J. Sustain. Aviat. 2 (2016) 181–202.
[3] P. Muzzell, L. Stavinoha, R. Chapin, Synthetic Fischer-Tropsch (FT) JP-8/JP-5 Aviation Turbine Fuel Elastomer Compatibility, 2005, p. 41.
[4] Y. Liu, C.W. Wilson, S. Blakey, T. Dolmansley, Elastomer compatibility test of alternative fuels using stress-relaxation test and FTIR spectroscopy, Proc. ASME Turbo Expo (2011) 1–11.
[5] B. Musil, B. Demmel, A. Lion, M. Johlitz, A contribution to the chemomechanics of elastomers surrounded by liquid media: continuum mechanical approach for parameter identification using the example of sorption experiments, J. Rubber Res. 24 (2021) 271–279, https://doi.org/10.1007/s42464-021-00093-9.
[6] R.J. Gormley, D.D. Link, J.P. Baltrus, P.H. Zandhuis, Interactions of jet fuels with nitrile O-rings: petroleum-derived versus synthetic fuels, Energy Fuel. 23 (2009) 857–861, https://doi.org/10.1021/ef8008037.
[7] J.L. Graham, R.C. Striebich, K.J. Myers, D.K. Minus, W.E. Harrison, Swelling of nitrile rubber by selected aromatics blended in a synthetic jet fuel, Energy Fuel. 20 (2006) 759–765, https://doi.org/10.1021/ef050191x.
[8] A.E. Mathai, S. Thomas, Transport of aromatic hydrocarbons through crosslinked nitrile rubber membranes, J. Macromol. Sci. Phys. 35 (1996) 229–253, https://doi.org/10.1080/00222349608212383.
[9] A. Blivernitz, T. Förster, S. Eibl, Simultaneous and time resolved investigation of diffusion processes of individual model fuel components in acrylonitrile-butadiene-rubber in the light of swelling phenomena, Polym. Test. 70 (2018) 47–56, https://doi.org/10.1016/j.polymertesting.2018.06.021.
[10] J. Liu, X. Li, L. Xu, P. Zhang, Investigation of aging behavior and mechanism of nitrile-butadiene rubber (NBR) in the accelerated thermal aging environment, Polym. Test. 54 (2016) 59–66, https://doi.org/10.1016/j.polymertesting.2016.06.010.
[11] J. Zhao, R. Yang, R. Iervolino, B. van der Vorst, S. Barbera, The effect of thermo-oxidation on the continuous stress relaxation behavior of nitrile rubber, Polym. Degrad. Stabil. 115 (2015) 32–37, https://doi.org/10.1016/j.polymdegradstab.2015.02.013.

[12] G.S. Buckley, C.M. Roland, Influence of liquid media on lifetime predictions of nitrile rubber, J. Appl. Polym. Sci. 131 (2014), 40296, https://doi.org/10.1002/app.40296.
[13] S. Akhlaghi, A.M. Pourrahimi, M.S. Hedenqvist, C. Sjöstedt, M. Bellander, U. W. Gedde, Degradation of carbon-black-filled acrylonitrile butadiene rubber in alternative fuels: transesterified and hydrotreated vegetable oils, Polym. Degrad. Stabil. 123 (2016) 69–79, https://doi.org/10.1016/j.polymdegradstab.2015.11.019.
[14] J. Zhao, R. Ynag, R. Iervolino, S. Barbera, Changes of chemical structure and mechanical property levels during thermo-oxidative aging of NBR, Rubber Chem. Technol. 86 (2013) 591–603, https://doi.org/10.5254/RCT.13.87969.
[15] J. Zhao, R. Yang, R. Iervolino, S. Barbera, Investigation of crosslinking in the thermooxidative aging of nitrile-butadiene rubber, J. Appl. Polym. Sci. 132 (1–5) (2015), 41319, https://doi.org/10.1002/app.41319.
[16] M. Celina, J. Wise, D.K. Ottesen, D.K. Gillen, R.L. Clough, Oxidation profiles of thermally aged nitrile rubber, Polym. Degrad. Stabil. 60 (1998) 493–504.
[17] R. Nevshupa, L. Martínez, L. Álvarez, M.F. López, Y. Huttel, J. Méndez, E. Román, Influence of thermal ageing on surface degradation of ethylene-propylene-diene elastomer, J. Appl. Polym. Sci. 119 (2011) 242–251, https://doi.org/10.1002/app.32519.
[18] R.J. Pazur, J.G. Cormier, K. Korhan-Taymaz, The effect of acrylonitrile content on the thermo-oxidative aging of nitrile rubber, Rubber Chem. Technol. 87 (2014) 53–69, https://doi.org/10.5254/rct.13.87937.
[19] R.J. Pazur, T. Mengistu, Activation energies of thermo-oxidized nitrile rubber compounds of varying acrylontrile content, Rubber Chem. Technol. 92 (2019) 129–151, https://doi.org/10.5254/rct.18.82592.
[20] S.S. Scheuermann, S. Forster, S. Eibl, In-depth interpretation of mid-infrared spectra of various synthetic fuels for the chemometric prediction of aviation fuel blend properties, Energy Fuel. 31 (2017) 2934–2943, https://doi.org/10.1021/acs.energyfuels.6b03178.
[21] A. Zschocke, S. Scheuermann, J. Ortner, High Biofuel Blends in Aviation (HBBA), Report, 2012. https://ec.europa.eu/energy/sites/ener/files/documents/final_report_for_publication.pdf.
[22] M.J. DeWitt, E. Corporan, J. Graham, D. Minus, Effects of aromatic type and concentration in Fischer-Tropsch fuel on emissions production and material compatibility, Energy Fuel. 22 (2008) 2411–2418, https://doi.org/10.1021/ef8001179.
[23] DIN 53504: Testing of Rubber – Determination of Tensile Strength at Break, Tensile Stress at Yield, Elongation at Break and Stress Values in a Tensile Test, Beuth Verlag, Berlin, 2009.
[24] J. Crank, The Mathematics of Diffusion, second ed., Clarendon Press, Oxford, 1975 https://doi.org/10.1016/0306-4549(77)90072-X.
[25] A. Blivernitz, Untersuchung der Verträglichkeit von Elastomeren mit synthetischen Flugturbinenkraftstoffen anhand ablaufender Diffusionsprozesse, PhD Thesis, Universität der Bundeswehr München, 2019.
[26] DIN 53765: Thermische Analyse Dynamische Differenzkalorimetrie (DDK), 1994.
[27] DIN ISO 48-4:2021-02: Rubber, Vulcanized or Thermoplastic – Determination of Hardness – Part 4: Indentation Hardness by Durometer Method (Shore Hardness) (ISO 48-4:2018), 2021, p. 26.
[28] S. Bhattacharjee, A.K. Bhowmick, B.N. Avasthi, Degradation of hydrogenated nitrile rubber, Polym. Degrad. Stabil. 31 (1991) 71–87.
[29] P.J. Flory, J. Rehner, Statistical mechanics of crosslinked polymer networks II, Swelling, J. Chem. Phys. 11 (1943) 521–526, https://doi.org/10.1063/1.1723792.
[30] G. Kraus, Degree of cure in filler-reinforced vulcanizates by the swelling method, Rubber Chem. Technol. 135 (1956) 928–951.
[31] M. Gauthier, W. Li, L. Tichagwa, Hard sphere behaviour of arborescent polystyrenes: viscosity and differential scanning calorimetry studies, Polymer (Guildf) 38 (1997) 6363–6370, https://doi.org/10.1016/S0032-3861(97)00202-4.
[32] J.S. Vrentas, C.M. Vrentas, Solvent self-diffusion in crosslinked polymers, J. Appl. Polym. Sci. 42 (1991) 1931–1937, https://doi.org/10.1002/app.1991.070420716.
[33] J.L. Valentín, A. Rodríguez, A. Marcos-Fernández, L. González, Dicumyl peroxide cross-linking of nitrile rubbers with different content in acrylonitrile, J. Appl. Polym. Sci. 96 (2005) 1–5, https://doi.org/10.1002/app.20615.
[34] K.F. El-Nemr, Effect of different curing systems on the mechanical and physico-chemical properties of acrylonitrile butadiene rubber vulcanizates, Mater. Des. 32 (2011) 3361–3369, https://doi.org/10.1016/j.matdes.2011.02.010.
[35] P.H. Starmer, Swelling of nitrile rubber vulcanizates-Part 3: factors affecting maximum swelling, J. Elastomers Plastics 25 (1993) 188–215, https://doi.org/10.1177/009524439302500302.
[36] V. Lachat, V. Varshney, A. Dhinojwala, M.S. Yeganeh, Molecular origin of solvent resistance of polyacrylonitrile, Macromolecules 42 (2009) 7103–7107, https://doi.org/10.1021/ma901336q.
[37] T. Förster, A. Blivernitz, Migration of mineral oil in elastomers, J. Rubber Res. 24 (2021) 257–269, https://doi.org/10.1007/s42464-021-00087-7.
[38] P.R. Morrell, M. Patel, A.R. Skinner, Accelerated thermal ageing studies on nitrile rubber O-rings, Polym. Test. 22 (2003) 651–656, https://doi.org/10.1016/S0142-9418(02)00171-X.
[39] P. Budrugeac, Accelerated thermal ageing of nitrile-butadiene rubber under air pressure, Polym. Degrad. Stabil. 47 (1995) 129–132, https://doi.org/10.1016/0141-3910(94)00101-D.
[40] K. Loos, A. Blivernitz, B. Musil, T. Rehbein, M. Johlitz, A. Lion, Challenges in Material Modelling and Testing of Elastomers, Int. Rubber Conf., London, 2019.
[41] G.R. Hamed, J. Zhao, Tensile behavior after oxidative aging of gum and black-filled vulcanizates of SBR and NR, Rubber Chem. Technol. 72 (1999) 721–730, https://doi.org/10.5254/1.3538829.
[42] K. Cho, W.J. Jang, D. Lee, H. Chun, Y. Chang, Fatigue crack growth of elastomers in the swollen state, Polymer (Guildf) 41 (2000) 179–183, https://doi.org/10.1016/S0032-3861(99)00142-1.